IEEE Access
Multidisciplinary ⋮ Rapid Review ⋮ Open Access Journal

Received 10 June 2024, accepted 14 July 2024, date of publication 22 July 2024, date of current version 7 August 2024.

Digital Object Identifier 10.1109/ACCESS.2024.3431941

RESEARCH ARTICLE

Mitigation of Colorimetric Variabilities in Smartphone-Assisted Diagnostic Reader Using Domain-Adaptation

SUNITA BHATT[1], SANDEEP KUMAR SINGH[1], SUNIL KUMAR[1], SUDIP KUMAR DATTA[2], AND SATISH KUMAR DUBEY[1]

[1]Centre for Sensors, Instrumentation and Cyber-Physical Systems Engineering (SeNSE), Indian Institute of Technology Delhi, New Delhi 110016, India
[2]Department of Laboratory Medicine, All India Institute of Medical Sciences, New Delhi 110029, India

Corresponding author: Satish Kumar Dubey (satishdubey@sense.iitd.ac.in)

This work was supported in part by the Science and Engineering Research Board, New Delhi, India, under Grant CRG/2021/006969.

ABSTRACT Urinary albumin is an excellent marker for the diagnosis of chronic kidney disease. Smartphone assisted accessory-free analyzers are gaining popularity in the quantification of urinary albumin in point-of-care settings, though, presently, they are widely used as a screening tool. Application of smartphone-based colorimetry systems are limited because they suffer from several operating problems such as camera settings and illumination conditions, that can change the colorimetric values. In addition, they suffer from the problem of domain shift i.e. extreme performance degradation when tested data (source) was captured in a setting different from that of the training (target) data. In this work, the problem introduced due to smartphone camera settings and illumination conditions, has been addressed by applying a domain adaptation deep learning method. It is the amalgamation of a generative model and convolutional neural network. Images captured using an iPhone under 3500K light conditions were used as the target dataset and other domains including different smartphones and light conditions were utilized as source datasets. Given test data from the source, its 'closest clone' was derived using generative model-based Pix2pixGAN and mapped to the target data. Further, a customized CNN model was used for the classification of the closest clone data. The proposed method yields an accuracy of ∼88% for inter-phone repeatability on test data. The efficacy of the proposed model was also evaluated under different illumination conditions.

INDEX TERMS Point-of-care (PoC) diagnosis, urinalysis, smartphone, domain adaptation, CNN.

I. INTRODUCTION

Chronic Kidney Disease (CKD) has become a leading cause of mortality in the older population due to diabetes mellitus and hypertension, and in the younger population as well due to various reasons such as obesity and lifestyle [1]. Various studies in recent years have shown a drastic increase in the total number of patients, and worldwide an estimated 843.6 million individuals are affected due to CKD [2], [3], [4]. Hence, diagnosis, screening, and monitoring of CKD have become of utmost importance. CKD diagnosis is generally done in laboratory settings, and various diagnostic tools such as glomerular filtration rate (GFR), or the presence of albumin or creatinine or their combination are tested in urine samples [5]. However, GFR, a tool to measure kidney function, is often normal or partially elevated in the early stages (stages 1 and 2). Although several studies have shown that microalbuminuria is a strong marker for the detection of early kidney damage, its detection is limited to laboratory settings only [6], [7]. Early-stage kidney disease diagnosis is essential for better health monitoring of diabetic patients as this disease is asymptomatic in stage one and stage two of its progression. There are standard methods to determine the concentration of albumin using immunoturbidimetry, nephelometer, flow injection analysis (FIA), and sequential injection analysis (SIA) yielding accurate results [8]. However, these systems are not portable and are typically used in central laboratory facilities. Studies have shown that traces of albumin in the

The associate editor coordinating the review of this manuscript and approving it for publication was Vishal Srivastava.

urine can be detected using the dipstick method which is a very cost-effective solution and can be very helpful, especially in remote settings [9], [10]. Urine dipsticks contain multiple sensor/ detection pads impregnated with different chemicals/reagent, that exhibit the change in their color when subjected to a specific analyte [9]. In colorimetry, the color of the sensor pads on urine dipstick changes with the concentration of analytes present in the sample. Changes in color values are assessed to estimate the concentration of the analyte. Typically, the color change is visually compared to the reference chart as shown in Fig. 1. Concentration of the albumin in the sample is accordingly labeled depending upon the color intensity of the detection pad. However, dipsticks are less sensitive at lower concentrations (<300 mg/L), which are clinically significant for the early diagnosis of CKD [9]. In addition, the interpretation of color using a reference color chart is subjective due to variation in visual perception of individuals. In addition, low sensitivity and specificity of dipstick methods impose a major hindrance to its widespread adoption [10].

There has been significant development in the field of smartphone-based optical readers for the quantitative estimation of analytes in urine due to their portability and ease of deployment in low-resource settings. Several research groups are working towards the development of smartphone-based sensing platforms for biomarker detection [11], [12], [13], [14], [15]. In most smartphone-based systems, the images of the urine dipsticks are captured using the camera of the smartphone, and color features are extracted. The change in the color values is quantified and categorized in multiple groups and analyte concentrations are estimated and classified using different image processing tools and classifiers [15], [16]. Despite many advantages of the smartphone-based systems, change in their performance with ambient lighting conditions, camera settings, and spectral sensitivity of the sensor, hinder their applicability [15]. Few research groups had addressed the issue of ambient illumination by using and an add-on device to the smartphones to illuminate and capture the images of urine dipsticks [16], [17], [18], [19]. Lee et al. demonstrated a smartphone app 'NutriPhone' that comprises a smartphone accessory, and a lateral flow test strip that quantifies vitamin B12 levels [17]. Srinivasan et al. integrated a smartphone with a disposable test strip to quantify the concentration of serum ferritin using fingertip blood [18]. Kim et al. used a smartphone camera to capture microfluidic channel images to quantify blood haematocrit [19]. These studies utilized customized 'black boxes' to avoid ambient light conditions and image blurring. However, these 'add-on' devices are smartphone-dependent and require customizing based on smartphone models.

To address this problem, researchers have implemented various approaches to quantify analyte concentration based on the accessory-free method. Table 1 outlines diverse methods employed for system calibration, encompassing: 1) Utilization of a reference color chart with image processing algorithms [20], 2) Application of color space transformation [21], [22], and 3) Incorporation of machine learning and deep learning classifiers [23], [24]. Researchers have used reference charts and color space transformations for calibration to render these systems accessory-free [21], [23]. However, it is important to note that these systems require calibration at every stage, taking into account fluctuations in lighting conditions specific to each type of smartphone. Additionally, uniform illumination across the strip and the control object is not guaranteed and further contributes to varying mean color values for both the control object and the strip [15], [24]. However, the performance of such sensors may differ with changes in illumination conditions and the smartphone models due to changes in the camera sensors and their settings such as focus, shutter speed, exposure, image signal processing (ISP), pipelines, and color temperature [25].

Emerging research has shown that machine learning has the potential to solve issues associated with ambient light conditions and camera settings [15], [28], [29]. Solmaz et al. Proposed SVM and Random Forest for the quantification of hydrogen peroxide using colorimetry test strip [24]. Bhatt et al. demonstrated different machine learning models: logistic regression, KNN, Random Forest, and Support vector machine (SVM) to quantify albumin in urine samples using paper-based strips [29]. Thakur et al. used a deep learning-based CNN model for automatic segmentation and quantification of albumin concentrations using urine strips [15]. In the studies, researchers have demonstrated machine learning models to mitigate ambient light conditions. However, when the same models were used for testing instead of training, accuracy decreased drastically. In addition to ambient light conditions, a shadow of the smartphone over the image was identified as a contributing factor to the suboptimal performance of the classification models [29]. In our study, this factor was taken care of using 'Flash on' mode of the smartphone that mitigates the shadow of a smartphone over the images [15].

Additionally, the spectral sensitivity of the camera may vary with smartphone models and therefore can affect the colorimetric value of images. Also, the pictures taken with diverse smartphone cameras may not faithfully represent the actual colors in the image, attributed to fluctuations in the light source's power distribution that alter colorimetric values. In interesting studies, the human ability of color perception was mimicked using a camera, one of the studies utilized a statistics-based algorithm wherein statistical algorithms impose priors [31]. In the second study, a learning-based algorithm was employed that relies on a training set [32]. It employs machine learning and Convolutional Neural Networks (CNN) for the classification and quantification of analytes [33].

This model performs well when CNN models are trained under controlled conditions (target), for example, the data was captured using a single camera sensor in specific illumination conditions. However, the classification performance degrades when confronted with diverse conditions (source) involving different camera sensors and illumination conditions. The shift in the domain from source to

TABLE 1. Smartphone-based point-of-care devices.

S. No	analyte	year	color space	strips	detection principle	algorithm	LOD	reference
1	Albumin	2016	HSV	Paper and cuvette	Images of the strip and the samples were simultaneously captured in a single shot by a digital camera on a mobile phone	Albumin smart test self-calibration approach	-	[21]
2	12 biomarkers	2017	RGB	Dipstick	Automatic localization of color pad and quantification concentration based on color feature	Reference chart Machine learning	-	[20]
3	Glucose protein	2017	lab	dipstick	Add-on device used to control light conditions	Calibrate with background	400, 60 mg/L	[16]
4	Alcohol	2017	RGB, HSV, YUV, and Lab	Paper strips	A smartphone was used to capture the alcohol test-strip image. Four color spaces were used to estimate the concentration using ML.	linear discriminant analysis (LDA), support vector machine, artificial neural network (ANN)	-	[26]
5	pH	2017	RGB	Paper-strips	Color-feature used for classification.	least-squares support vector Machine	-	[23]
6	Hydrogen peroxide	2018	RGB, HSV, lab	Dipsticks	Accessory-free smartphone used to quantify hydrogen peroxide	Machine learning	-	[24]
7	Antigen	2019	HSV	96 well plate	Saturation in HSV used to control ambient light conditions	Color-Calibration	-	[22]
8	Albumin	2020	RGB, HSV, lab	Paper-based strips	RF algorithm was used to classify concentrations	Random Forest (RF)	750 mg/L	[15]
9	pH, proteins, and glucose	2021	RGB, HSV	Paper-strips	Urine test strips, based on the CIE-xy nearest neighbor algorithm. Four illuminations were explored in the range of 100 -400 lx.	CIE-xy nearest neighbor	75 mg/L	[27]
10	Glucose	2021	RGB, HSV, lab	Paper-strips	Mean skewness and kurtosis, contrast, correlation, homogeneity and energy, entropy, and intensity are calculated.	Machine learning-based gradient boosting classifier	47 µM	[28]
11	Albumin	2023	RGB, HSV, lab	urine strips	Color spaces were used to estimate concentration using a kNN algorithm	K-Nearest Neighbor (kNN)	4 mg/L	[29]
12	Albumin	2023	RGB	Paper-based dipstick	Add-on box attached consists of smartphone for illumination at 555nm and a sample. Another smartphone was used to capture images. Data is processed using ImageJ.	ImageJ used for the image process	70 mg/L	[30]

target causes a severe performance degradation in terms of accuracy which can be solved using the domain adaptation approach [34], [35]. These models, learns domain-invariant representations by employing the principles of adversarial learning. In pix2pixGAN model, pixel-wise learning was employed to learn pixel-wise transformation. The primary objective is defined as training a model that can take an input image and generate a corresponding output image with a desired attribute.

In this study, the authors propose a customized GAN concatenated CNN i.e. pix2GCNN model to classify albumin concentrations ranging from 1280 mg/L to 5 mg/L. The images of the urine dipstick were captured using four different smartphone cameras. Images captured using the iPhone SE smartphone model were served as targets. In the source dataset, images captured using other smartphones i.e. Redmi, Realme, and Samsung were utilized. Effectiveness of the model was also investigated under different illumination conditions using two different light sources i.e., a tungsten bulb

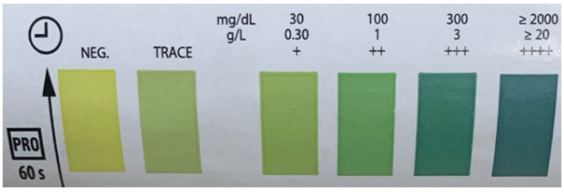

FIGURE 1. Reference color chart which comes with a commercially available urine dipstick that is used for protein concentration measurement; neg, trace, 300, 1000, and 20000 mg/L respectively.

corresponding to a color temperature of 3500K and compact fluorescence light having a color temperature 6500K. Here, the images captured at 3500K color temperature were used as the target dataset and images captured at 6500K were used as source dataset.

The pix2pixGAN model performs an image-to-image translation to learn the mapping between the source image and the target image. The pix2pixGAN was used to find the

'closest clone' images for source images that were arbitrarily close to the target images. The source images that belong to different spectral distributions (i.e. different domains) were replaced with its 'closest clone'' images. Finally, customized CNN was used to obtain the classes of albumin analytes. Dependence of the proposed model for different smartphone cameras was also investigated. A customized dataset generated using four different smartphones was used. Here, the images were captured at different illumination conditions and also at different color temperatures. All the images were captured in ''Flash ON'' mode of the camera to mitigate the effect of ambient light conditions. Issues related to domain shift were addressed using pix2GCNN technique that computes the 'closest-clone' of the source data for a given image and has been used for the classification of albumin concentrations. Performance of the proposed method was evaluated on various datasets obtained using different smartphone models i.e. iPhone SE, Redmi 8A Dual, Samsung Galaxy M01, and Realme C11 under various light conditions. The proposed model was also tested al lower concentrations (up to 5mg/L) as they are clinically significant but challenging to detect due to extremely less variation in the color values. These finding were also validated on the same dataset using Nephelometry, the gold-standard technique.

II. MATERIAL AND METHODOLOGY

This section outlines the stages involved in the classification of albumin concentration on a urine dipstick, including solution preparation, methodology, a customized generative pix2GCNN model, and assessment metrics. First, the human serum albumin was used to prepare the solution of albumin at different concentrations, ranging from 1280 to 10 mg/L, using serial dilution approach. Images were acquired using four different smartphones (iPhone, Redmi, Realme, Samsung) at two different color temperatures: 3500 K and 6500 K, to realize two different illumination conditions. The color parameters were extracted from these images. To mitigate the effect of the variations in the illumination conditions and the smartphone variability, 'closest clone' images were generated using the pix2pix model. Further albumin concentrations were classified using a customized CNN model. The complete image processing algorithm has been discussed in the methodology section.

A. SAMPLE PREPARATION AND DATASET

The standards used in the present study were synthesized at AIIMS, New Delhi under the supervision of a medical expert. The stock solution was prepared by dissolving 3.2 mg of solid powder of human serum albumin (HSA) in 2.5 ml of water, yielding the albumin standard solution of 1280 mg/L concentration, termed as C1. The albumin solutions at eight other concentrations C2, C3, ...C9, corresponding to 640 mg/L, 320 mg/L, 160 mg/L, 80 mg/L, 40 mg/L, 20 mg/L, 10 mg/L, and 5 mg/L were prepared using the serial dilution approach by adding the proportionate amount of deionized water to the stock solution. The urine dipsticks were dipped in these solutions and

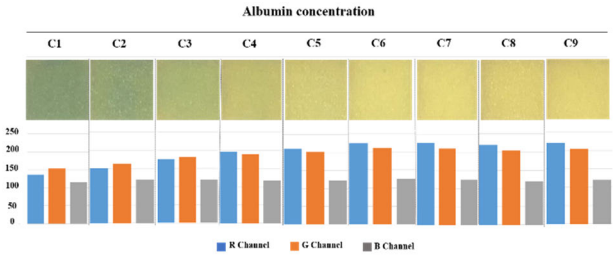

FIGURE 2. A bar plot has been added to show the variation of color parameters in RGB color space channels for nine different concentrations of albumin ranging from C1 (1280 mg/L) to C9 (5 mg/L).

respective images were captured using the smartphone camera to quantify the color changes corresponding to different albumin concentrations. The color variations at nine different concentrations are shown in Fig. 2. Concentrations of these standard solutions were validated on the same day using Nephelometer and immunoassay-based methods. Solutions within concentration range of 5 to 200 mg/L were validated using a nephelometer whereas immunoassay-based method was performed to validate the concentrations >200 mg/L.

To conduct this study, we have used nine different concentrations of albumin. Four different smartphones (Redmi, Realme, Samsung and iPhone) were used to capture the images at two different light source corresponds to color temperatures; 3500 K and 6500 K. At each color temperature, six different illuminance conditions; 500 Lux, 400 Lux, 300 Lux, 200 Lux, 100 Lux, and 50 Lux at the sample plane were realized by changing the angle of incidence of the light source. Four images were captured at each concentration using a specific smartphone camera leading to a total of 36 images, corresponding to 9 different concentrations, using a single smartphone at a specific illuminance value (e.g. 500 Lux) at the sample plane at a specific color temperature (e.g. 3500 K). In this manner, total of 1728 images (36*6*4*2) were captured at all the 6 illuminance values at the sample plane using 4 different smartphone cameras at two different color temperatures. In each study, the entire dataset was split into 80:20 for training and validation purposes. Further, the model was used to test an unseen dataset. For training the model, data augmentation was performed through flip, rotation, and zoom operations to increase the volume of the data for the robust learning of the model. Total 27648 images were created by applying the data augmentation operation which further split into 80:20 ratios for train and validation i.e. 22119 and 5529 images respectively. Further, the 216 images that were captured at 6 different illuminance values, using single smartphone at the color temperature of 3500 K, that belongs to unseen data, were used for testing the model.

B. METHODOLOGY

The colorimetric value of any image/object is affected due to the following factors: 1) Change in image sensing device

such as smartphone, 2) Variation in light conditions such as illumination and color temperature, 3) Angle introduced in image or sensor. Here, we have used smartphones to capture images of urine dipsticks. Albumin samples were introduced onto the chemically impregnated dipsticks for 10 seconds leading to change in color value of the sensor pad at the strip. Images of dipsticks were captured using a smartphone camera after 60 seconds, allowing the chemical reaction to complete. The ambience color temperature was maintained at 3500K using a tungsten bulb. The illumination at the strip was varied by changing the angle of the light source leading to resultant luminance in the range of 500 Lux to 50 Lux. Four images of individual concentrations were taken for the repeatability of the process. The above process was repeated for all albumin concentrations ranging from C1 to C9. These studies were repeated using different smartphone cameras i.e iPhone SE, Redmi 8A Dual, Realme C11, Samsung Galaxy M01. The colorimetry values of images are affected due to variations in the spectral sensitivity of the smartphone camera and changes in the intensity of the ambient light condition as shown in Fig.3. Here, this problem was addressed using the domain adaptation method i.e. the pix2pixGAN model [37], [38], [39]. This model consists of two parts: a generator and a discriminator, which is simultaneously trained, as shown in Fig. 4. The generator produces synthetic data that is cloned to the real data, while the discriminator tries to distinguish between the real data and the synthetic data. Fig. 5 presents the proposed methodology to classify albumin concentrations using GAN model. Here, the images acquired in all the studies using an iPhone were labeled as the target domain. The pix2pix model acquires detailed pixel-level information to effectively translate images from the source to the target domain. Once the domain shift problem was mitigated, customized CNN model was used for the classification of concentrations as discussed in section C. Here it was noticed that the CNN model was trained only using target images and tested on 'closest-clone' images that belong to different source domains (different smartphone models). The performance of the model has been discussed in detail in section III. To ensure the robustness of the model, a series of studies were conducted using different smartphone models: Realme and Samsung. In addition, the effectiveness of the model was also evaluated by introducing different light conditions i.e. compact fluorescent lamp (CFL, color temperatures: 6500K).

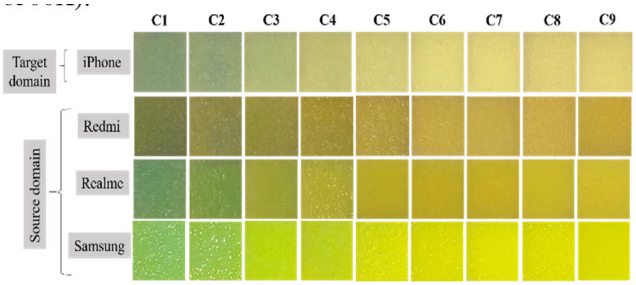

FIGURE 3. Albumin sensor pad of nine different concentrations (1280 mg/L to 5 mg/L) showing the variation in color with different domain images captured using smartphone sensors using 'Flash on' mode.

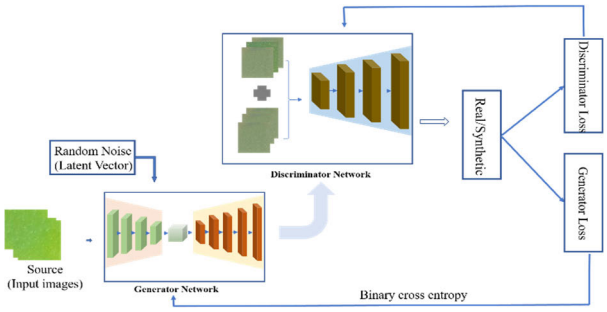

FIGURE 4. Block diagram of Pix2pixGAN architecture. Input is an albumin detection pad captured using smartphone models.

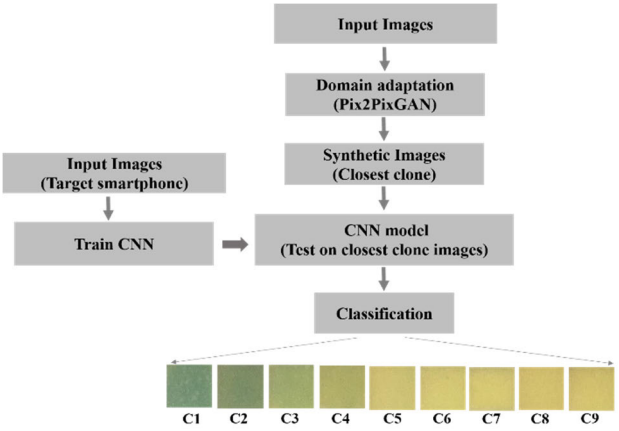

FIGURE 5. Block diagram of proposed methodology to classify albumin concentration ranging from C1 to C9 using Domain Adaptation method.

C. GENERATIVE PIX2GCNN MODEL

In this study, we have demonstrated the utilization of a generative model equipped with a deep classifier. The generative model (pix2pixGAN) has been concatenated with customized CNN model. In pix2pixGAN model, a generator is based on U-net network with convolutional layers to extract the features from input images [39]. Convolution and pooling layers progressively decrease the spatial dimension which follows the expansion path where convolution and up-sampling layers amplify spatial dimensions while reducing feature maps. In addition, skip connections are employed for high-resolution information preservation from the input images. The generator is designed to adhere to a discriminator which was trained to differentiate between real and generated image pairs [40]. During training, the generator is trained to minimize the difference between the generated output image and the ground truth output image, while the discriminator is trained to differentiate between real and generated image pairs. Here, we computed the final loss as a combination of adversarial loss and L1 function as given by equation 1. The reason for using L1 loss instead of L2 loss was based on the observation that it resulted in less blurred output images.

$$G^* = argminmaxL_{cGAN}\,(G, D))+\lambda L_{l1}(G) \qquad (1)$$

Algorithm 1 Customized CNN

Input: **Group of images**

Output = class of input image

for *train data:*
Compute feature maps for input image using kernel filter w as below
$\mathbf{X} = \boldsymbol{x}^{l-1} * \boldsymbol{W}^{l}$, where 1 is no of filters.
High dimension images follow max pooling for down sampling as
$\boldsymbol{y} = \boldsymbol{max}_{i,j=1}^{h,w} \boldsymbol{X}_{i,j}$
The probability of output class will calculate using the Softmax function
$\sigma(y) = \frac{e^{y}}{\sum e^{y}}$
end for
Predict output based on the trained model on test data

where, λ is a hyperparameter that specifies the weight of L1 error (λ = 100), and l_1 loss applied on the generator as the difference between the generated image and the ground truth image defined in equation 2. L_{cGAN} is an adversarial loss which is based on the sigmoid cross-entropy loss. It measures the ability of the generator to fool the discriminator into classification of the generated image as real images.

$$L_{l1} = E_{x,y,z}[|y - G(x,z)|_1] \tag{2}$$

where, x is input data, y is target data, z is random vector, and G (x, z) is Generated output image.

The generated image produced by the Pix2pixGAN model was used for feature-wise normalization and sample-wise normalization and passed to the CNN architecture to classify nine different concentrations of albumin analyte. The CNN model consists of five convolution layers, three max-pooling layers, one fully connected layer, and a softmax layer as the output layer as shown in Fig. 6.

Each image was resized to 128 × 128 × 3 pixels, to reduce the computational burden, and input features as RGB color space. The kernel size was set as 3 × 3. After the convolution layer, the max pool layer with kernel size 2 × 2 was used to select feature values with nine classes. For weight initialization "random-normal" was used along with "Adam" optimizer with a learning rate of 0.001. The proposed model is smaller with less convolution layer which consumes less time and can be easily integrated with smartphone devices. The pseudo-code for the proposed CNN model is given in algorithm 1.

D. EVALUATION METRICS

The performance of the pix2pixGAN model was evaluated using two parameters 1. Structure Similarity Index (SSIM) and 2. Root Mean Square Error (RMSE). In calculating the SSIM score, it is considered that the human visual system is highly adapted to extract structural information from an image [41]. It follows that a structural information

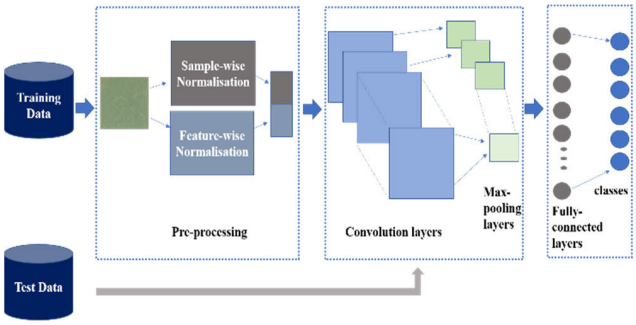

FIGURE 6. The proposed customized Convolution Neural Network (CNN) for the classification of all nine concentrations of albumin. A pre-processing layer was added to extract most prominent feature from input images.

measurement change can provide a good approximation for image quality. It compares local patterns of pixel intensities for luminance and contrast. It is defined as:

$$SSIM = \frac{(2\mu_x\mu_y + c_1)(2\sigma_{xy} + c_2)}{(\mu_x^2 + \mu_x^2 + c_1)((\sigma_x^2 + \sigma_x^2 + c_2)}\ (3) \tag{3}$$

where μ_x and μ_y are average of x and y, σ_x^2 and σ_y^2 are variance of x and y, σ_{xy} is the covariance of x and y. c_1 and c_2 are constant defined as; $c_1 = (k_1 L)^2$ and $c_2 = (k_2 L)^2$, L is known as dynamin range and k_1, k_2 are constants ($k_1 = 0.01, k_2 = 0.03$). The RMSE is a well-known image quality estimator that is used to calculate the difference between the predicted value and the ground truth value. A value close to zero is referred as a better-quality image. The RMSE between two images is defined as:

$$RMSE = \sqrt{\frac{1}{NM}} \sum_{i=1}^{N} \sum_{j=1}^{M} (x_{ij} - y_{ij})^2 \tag{4}$$

The CNN performance of classification was evaluated using four metrics i.e. accuracy, precision, recall, and f1-score. These functions are defined as follow:

$$Accuracy = \frac{(TP + TN)}{D} \quad Precision = \frac{TP}{(TP + FP)}$$
$$Recall = \frac{(TP)}{(TP + FN)} \quad F1 - score = \frac{2}{\left(\frac{1}{Precision} + \frac{1}{recall}\right)}$$

where, TP: True Positive, TN: True Negative, FN: False Negative, FP: False Positive, D: Total data points. In addition, confusion metrics were depicted for all experiments. These metrics demonstrate how accurately the model predicts the data points.

III. RESULT AND DISCUSSION

In this study, customized pix2pixGAN model was used for domain adaptation. Source data, referred as input data, was collected using different smartphones. The target data was collected using iPhone. Pairwise data from the source and target were fed to the model. Performance of the proposed model was evaluated using the source data from different smartphone models; Redmi 8A Dual, Samsung Galaxy M01,

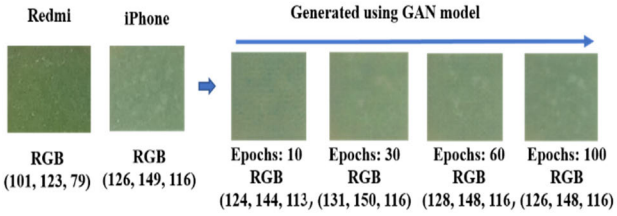

FIGURE 7. The change in RGB color values of GAN generated images at different epochs such as 10, 30, 60, and 100. Redmi and iPhone images were used as source and target data respectively (left to right).

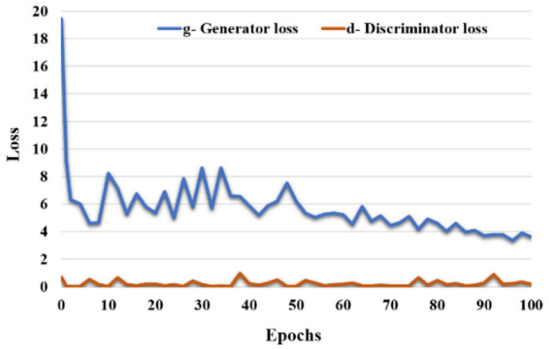

FIGURE 8. Loss functions with 100 epochs to train pix2pixGan for source(iPhone) and target (Redmi) data captured at all nine concentrations.

and Realme C11. A total of 100 epochs with 216 batch sizes were optimized to train the model. The 'closest clone' of the target corresponding to the source was achieved at the output of the model. The R, G, and B color values of outputs at discrete epochs such as 10, 30, 60, and 100 epochs were collected as shown in Fig. 7. It was observed that at 100 epochs the RGB value (126, 148, 116) of the 'closest clone' closely resembles the desired target image value of (126, 149, 116). Since the discriminator learns faster than the generator, the loss corresponding to the discriminator was lower than a generator. Also, at 100^{th} epoch, both the losses exhibit saturation, indicating a plateau in individual progression as shown in Fig. 8. Images of the albumin patches at all nine concentrations, corresponding to source, 'closest clone', and target are shown in Fig. 9. Significant difference was observed in the color values between the source and target data which was minimized using the proposed model. RGB values for these images were calculated after training the pix2pixGAN model. The calculated RGB values of 'closest clone' images closely matched with those of the target images, as shown in the comparison chart in Fig. 10.

There was a noticeable similarity in color values between the closest clone and the target images. In addition to color value, performance of the model was also evaluated by computing the RMSE and SSIM scores for all concentrations as shown in Fig 11 (a, b). Originally, the RMSE value was high as the data distribution between source and target was different. It was observed that the RMSE value for source and target data gets drastically reduced after applying the proposed model.

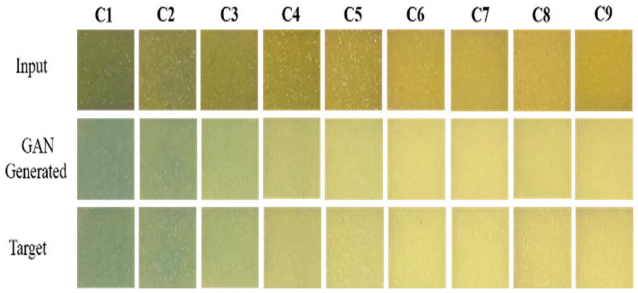

FIGURE 9. Albumin detection patch from urine dipstick for all nine concentrations i.e. C1 to C9 for three different domains.

On the other hand, the SSIM value between source and target images significantly increases after applying the proposed model. Therefore, it can be inferred that the pix2pixGAN model can be used to mitigate the problem of domain shift. Further, concentrations were classified into corresponding classes; C1 to C9 using a CNN model.

To train the CNN model, target data that was captured using iPhone and was split into 80:20 ratio as train and validation dataset. The loss for both train and validation decreases to 0.08 at 100 epochs. The train and validation accuracy were found to be ∼0.95 at 100 epochs. The trained CNN model was tested using unseen data that belongs to different domains. Both images; 'closest clone' and source data were utilized to evaluate the robustness of the model. Performance of the proposed CNN model was evaluated by computing different parameters on the original image (without pix2GCNN) and the one obtained after applying pix2pixGAN model. Table 2 shows the CNN performance between these two modes ''with pix2GCNN'' and ''without pix2GCNN'' model.

A total of 216 images, corresponding to all 9 concentrations were included in this study. It was observed that the accuracy of the proposed model gets enhanced drastically from 0.28 to 0.88 using ''closest-clone'' images. Other parameters such as precision, recall and f1-score also support this claim. The recall and f1-score parameters were found below 0.5 and 0.3 respectively for ''without pix2pixGAN'' mode which were improved using ''with pix2pixGAN'' mode. On the other hand, the performance of the model using 'with pix2GCNN' was significantly high for all images corresponding to different classes. The confusion matrix, as shown in Fig. 12, was derived to visualize the classification of the proposed model for all classes. The concentrations ranging from C1 to C9 correspond to 0 to 8. The diagonal elements represent the correct classes of data points corresponding to individual concentrations whereas off-diagonal elements represent the misclassified data points. It was found that almost all classes for ''without pix2GCNN'' were misclassified in Fig. 12(a) whereas, they were correctly classified for ''with pix2GCNN'' as shown in Fig. 12 (b). This demonstrates the effectiveness of pix2GCNN model in domain shifting problem, wherein the performance of model was enhanced without using source data during classification. Therefore, domain shift issue can be addressed effectively using pix2GCNN model, wherein, classification accuracy can be improved without the knowledge of source data.

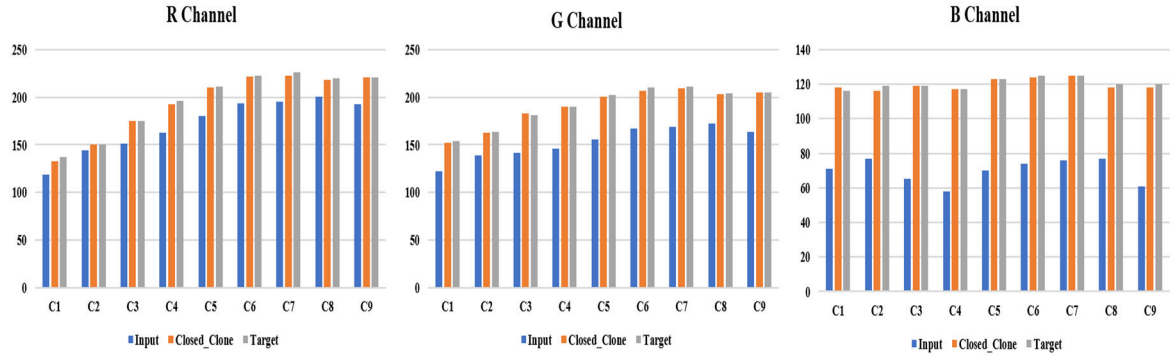

FIGURE 10. Color value comparison between input, 'closest clone', and target images. RGB value was calculated for the albumin detection pad after training the pix2pixGAN model for all nine classes.

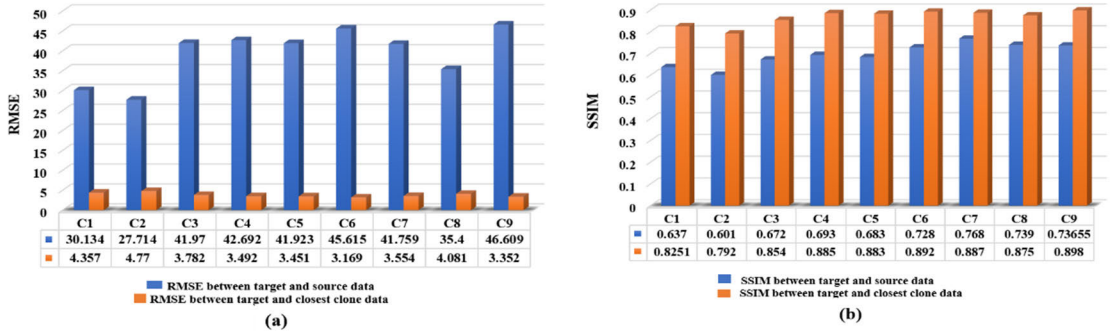

FIGURE 11. Performance evaluation of pix2pixGAN model using two parameters: (a) RMSE and (b) SSIM. Parameters were calculated between source data (Redmi) and target data (iPhone), 'closest-clone' (GAN generated) and target data.

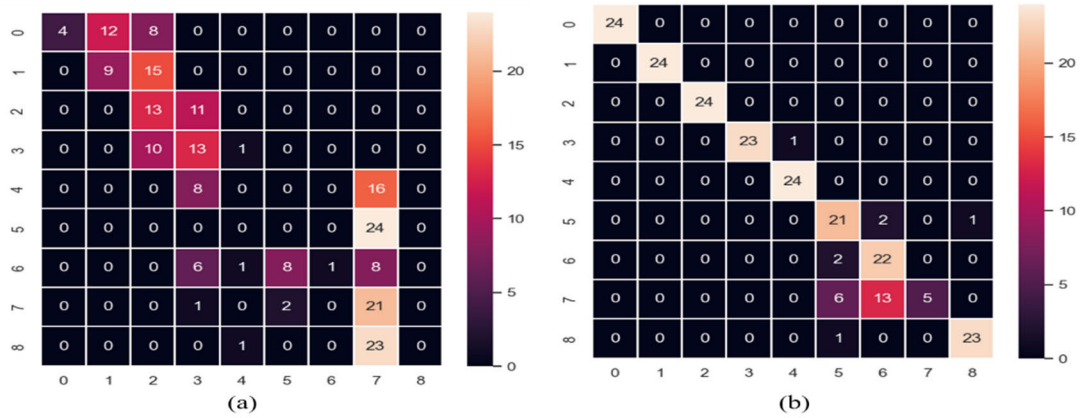

FIGURE 12. Confusion matrix for CNN classifier of all nine different classes using (a) source images, (b) 'closest-clone' images. In label, 0 to 8 denote the concentration from C1 to C9 respectively.

A. PERFORMANCE EVALUATION OF PIX2GCNN MODEL FOR VARYING SENSORS AND ILLUMINATION CONDITIONS

Performance of the proposed model (Pix2GCNN) was also evaluated on different smartphones and under different ambient illumination conditions to assess its robustness.

1) PERFORMANCE USING DIFFERENT SENSORS/SMARTPHONES

As discussed above, study of domain shift was performed by mapping the data from one camera sensor (Redmi smartphone) as the source to another camera sensor (iPhone) as the target. This study was further extended by using two more sources (smartphones); Realme and Samsung, while

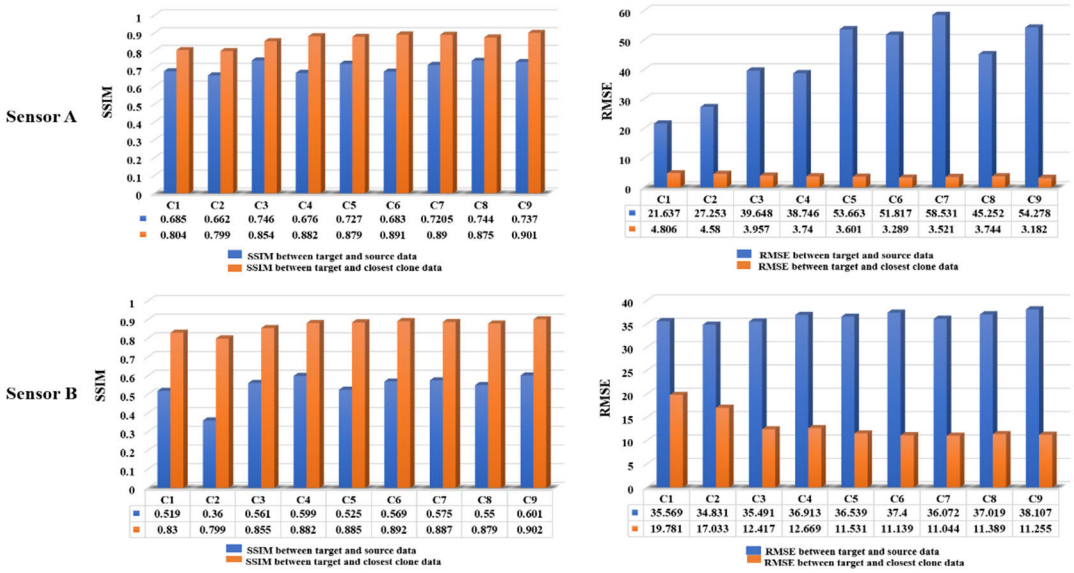

FIGURE 13. Performance evaluation of GAN model using two parameters: a) RMSE and b) SSIM. Values were calculated between target data (iPhone) and source data captured using sensor A and B, 'closest clone' (GAN generated) and target data.

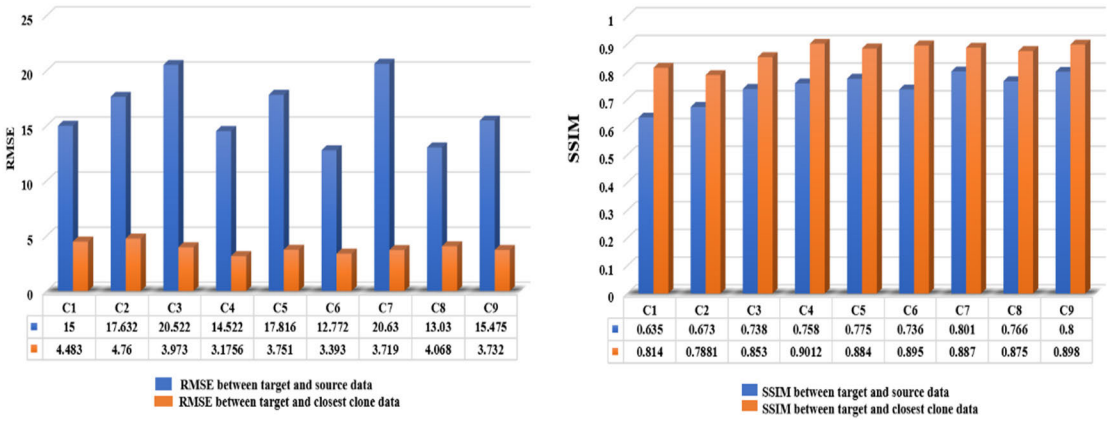

FIGURE 14. Performance evaluation of GAN model using two parameters: RMSE and SSIM. a) RMSE values calculated between target data (3500K) and input data captured under 6500K, closest clone (GAN generated) and target data. (b) SSIM comparison between all domain data.

TABLE 2. Comparison between 'Without pix2GCNN' and 'With pix2GCNN' dataset using evaluation parameters i.e. precision, recall, F1-Score, F1-Score and accuracy.

Parameters	Precision	Recall	F1-Score	Accuracy	Sample
Without pix2GCNN	0.36	0.28	0.21	0.28	216
With pix2GCNN	0.91	0.88	0.86	0.88	216

keeping the target (iPhone) fixed. Here, the images captured using the camera of the iPhone were used as target data which was trained for the classification of nine different classes. The images captured using the cameras of smartphones Redmi, Realme, and Samsung were used as the test data. The performance of the model using Redmi as the source data has been discussed in section III. Here, we present the feasibility of the model tested on Realme (sensor A) and Samsung (sensor B) smartphones after generating 'closest clone' images. Color values i.e. R, G, and B for input, 'closest clone', and target images were calculated for both sensors. Spectral sensitivity of sensors changes the colorimetric values of images. The change in color values were minimized using 'closest clone' images for all nine concentrations/classes. Performance matrices SSIM and RMSE were calculated using input, 'closest clone', and target data for camera sensors A and B at all concentrations, as shown in Fig. 13. The pixel-wise differences or errors were higher between source and target images as shown in RMSE which was further reduced using 'closest clone' data for both sensors

TABLE 3. Comparison between 'Without pix2GCNN' and 'With pix2GCNN' dataset using evaluation parameters i.e. precision, recall, F1-Score, F1-Score and accuracy for both sensors 'A' and 'B'.

Sensors	Parameters	Precision	Recall	F1-Score	Accuracy	Sample size
Sensor A	Without pix2GCNN	0.45	0.41	0.33	0.41	216
	With pix2GCNN	0.89	0.88	0.86	0.88	216
Sensor B	Without pix2GCNN	0.36	0.30	0.26	0.30	216
	With pix2GCNN	0.85	0.81	0.78	0.81	216

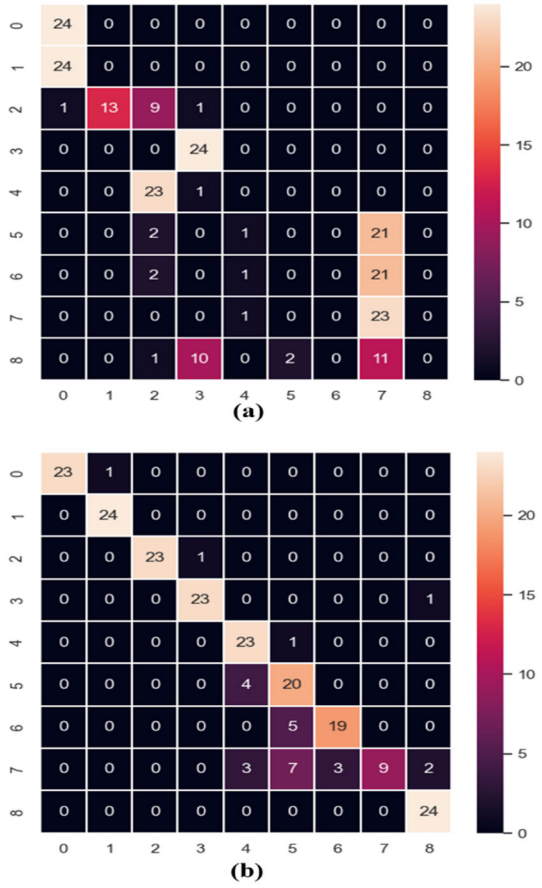

FIGURE 15. Confusion matrix for CNN classifier of all nine different classes using (a) source, and (b) 'closest clone' images.

A and B. It was noticed that there is a high SSIM between the 'closest clone' and target data. This demonstrates that the proposed model could address the issue of domain shift across the camera sensors. Further, the CNN model, which was already trained on the target data, captured using iPhone, was applied on the 'closest clone' data. The robustness of the model was evaluated by applying it on the original images (source images) and the closest clone images, captured using camera sensors A and B. It was observed that parameters; precision, recall, f1-score, and accuracy; were enhanced after applying the pix2pixGAN on the source data. For example, accuracy got changed from 0.41 to 0.88 and 0.30 to 0.81 for camera sensors A and B respectively, as shown in Table 3. Precision, recall, f1-score, and accuracy corresponding to all nine concentrations were calculated. A confusion matrix was computed to study the performance of the proposed model for all nine classes. It can be inferred that the proposed model is not limited to a specific smartphone camera sensor but works well across various smartphone models and therefore, its performance is nearly invariable to smartphone model.

2) DIFFERENT UNDER DIFFERENT AMBIENT LIGHT CONDITIONS

The above study was performed at two different color temperatures; 6500K and 3500K to understand its performance under different illumination conditions. Both source and target data were captured using the same smartphone camera. The model was trained on the target data captured using iPhone SE at 3500K color temperature and tested on the source data which was also captured using the camera of the same iPhone, but at different illumination conditions where the color temperature was kept at 6500K. The 'closest clone' of the target data corresponding to the respective source data was created using the pix2pixGAN model. The R, G, and B color values were extracted, and a comparison was made among the source data, the closest clone and the target data. As the intensity of the light varies with the color temperature, variation is perceived in the reflected colors from the albumin strips. Therefore, SSIM value was calculated for all the images i.e. source, closest clone and the target data, which is shown in Fig. 14. The CNN model was applied on both source and 'closest clone' data separately to classify the concentrations. Classification accuracy for 'closest clone' and source dataset was 87 % and 37 % respectively. The performance of the CNN model has been presented in confusion matrices in Fig. 15. In source data, almost all classes were misclassified, whereas they were correctly classified using 'closest clone' data as shown in Fig. 15 (a) and Fig. 15(b) respectively. Thus, the proposed model is robust enough to classify the concentrations in corresponding classes without the requirement of training the data every time.

IV. CONCLUSION

In the present study, concentrations of urinary albumin were estimated and classified using a smartphone-assisted, colorimetry-based diagnostic reader, using readily available urine dipsticks. Despite consistent illumination and ambient light conditions significantly influence the color values,

thus making it difficult to classify at lower concentrations. Variations in color temperature of light source can also alter the appearance of objects, potentially affecting colorimetry value of an image. In concentration analysis based on colorimetry, such variation in color value due to external factors can lead to misclassifications of concentration values. Further, significant variations are observed across different color spaces for different smartphone cameras that exhibit variations in spectral sensitivity. These variations may lead to incorrect interpretations of albumin concentration levels in urine samples. These colorimetric variabilities have been addressed using pix2pix generative model based on domain adaptation. The 'closest clone' images were generated using pix2pixGAN that mitigates the variability introduced using different sensors and light conditions. Quantification of albumin was done using a customized CNN model. The pix2pixGAN concatenated with CNN model yields the maximum accuracy of 88% as compared to 83%, reported in literature, on the test data, captured using different smartphone models at a fixed color temperature of 3500K. In addition, the proposed model exhibits a remarkable improvement in the classification accuracy on the test data captured at two different color temperatures; 3500K and 6500K. Performance of the proposed model was also studied by deriving the confusion metrics. The usefulness of the proposed method has been experimentally demonstrated on multiple modalities covering different smartphone sensors under different ambient light conditions. The proposed model has the potential to be incorporated into a mobile application that can be used for quantification and classification of different analytes in low-resource settings. As a future scope, it is planned to explore the feasibility of the proposed model on the clinical samples.

REFERENCES

[1] H. Wang, M. Naghavi, C. Allen, R. M. Barber, Z. A. Bhutta, A. Carter, D. C. Casey, F. J. Charlson, A. Z. Chen, M. M. Coates, and M. Coggeshall, "Global, regional, and national life expectancy, all-cause mortality, and cause-specific mortality for 249 causes of death, 1980–2015: A systematic analysis for the Global Burden of Disease Study 2015," *Lancet*, vol. 388, no. 10053, pp. 1459–1544, 2016.

[2] K. J. Jager, C. Kovesdy, R. Langham, M. Rosenberg, V. Jha, and C. Zoccali, "A single number for advocacy and communication-worldwide more than 850 million individuals have kidney diseases," *Nephrol. Dialysis Transplantation*, vol. 34, no. 11, pp. 1803–1805, 2019.

[3] W. G. Couser, G. Remuzzi, S. Mendis, and M. Tonelli, "The contribution of chronic kidney disease to the global burden of major noncommunicable diseases," *Kidney Int.*, vol. 80, no. 12, pp. 1258–1270, Dec. 2011.

[4] C. P. Kovesdy, "Epidemiology of chronic kidney disease: An update 2022," *Kidney Int. Supplements*, vol. 12, no. 1, pp. 7–11, Apr. 2022.

[5] J. A. Kellum, N. Lameire, P. Aspelin, R. S. Barsoum, E. A. Burdmann, S. L. Goldstein, C. A. Herzog, M. Joannidis, A. Kribben, A. S. Levey, and A. M. MacLeod, "Kidney disease: Improving global outcomes (KDIGO) acute kidney injury work group," *KDIGO Clin. Pract. Guideline Acute Kidney Injury. Kidney Int. Supplements*, vol. 2, no. 1, pp. 1–138, 2012.

[6] R. J. Glassock, "Is the presence of microalbuminuria a relevant marker of kidney disease?" *Current Hypertension Rep.*, vol. 12, no. 5, pp. 364–368, Oct. 2010.

[7] D. de Zeeuw, H.-H. Parving, and R. H. Henning, "Microalbuminuria as an early marker for cardiovascular disease," *J. Amer. Soc. Nephrol.*, vol. 17, no. 8, pp. 2100–2105, Aug. 2006.

[8] D. Kumar and D. Banerjee, "Methods of albumin estimation in clinical biochemistry: Past, present, and future," *Clinica Chim. Acta*, vol. 469, pp. 150–160, Jun. 2017.

[9] C. P. Wen, Y. C. Yang, M. K. Tsai, and S. F. Wen, "Urine dipstick to detect trace proteinuria: An underused tool for an underappreciated risk marker," *Amer. J. Kidney Diseases*, vol. 58, no. 1, pp. 1–3, Jul. 2011.

[10] S. L. White, R. Yu, J. C. Craig, K. R. Polkinghorne, R. C. Atkins, and S. J. Chadban, "Diagnostic accuracy of urine dipsticks for detection of albuminuria in the general community," *Amer. J. Kidney Diseases*, vol. 58, no. 1, pp. 19–28, Jul. 2011.

[11] Y. Bai, Q. Guo, J. Xiao, M. Zheng, D. Zhang, and J. Yang, "An inkjet-printed smartphone-supported electrochemical biosensor system for reagentless point-of-care analyte detection," *Sens. Actuators B, Chem.*, vol. 346, Nov. 2021, Art. no. 130447.

[12] H. Chen, Z. Zhuang, S. Guo, S. Xie, Y. Xin, Y. Chen, S. Ouyang, W. Zhao, K. Shen, J. Tao, and P. Zhao, "Artificial neural network processed linear-light tristimulus and hue parameters of fluorescence for smartphone assisted point-of-care testing device," *Sens. Actuators B, Chem.*, vol. 384, Jun. 2023, Art. no. 133659.

[13] L. Liang, Y. Jiang, F. Liu, J. Wu, L. Tian, S. Zhao, and F. Ye, "Smartphone flashlight-triggered covalent organic framework nanozyme activity: A universal scheme for visual point-of-care testing," *Sens. Actuators B, Chem.*, vol. 381, Apr. 2023, Art. no. 133422.

[14] W. Wu, D. Zhou, X. Chen, X. Tang, J. Jiang, L. Yu, H. Li, Q. Zhang, Z. Zhang, and P. Li, "Intelligent point-of-care test via smartphone-enabled microarray for multiple targets: Mycotoxins in food," *Sens. Actuators B, Chem.*, vol. 360, Jun. 2022, Art. no. 131648.

[15] R. Thakur, P. Maheshwari, S. K. Datta, S. K. Dubey, and C. Shakher, "Machine learning-based rapid diagnostic-test reader for albuminuria using smartphone," *IEEE Sensors J.*, vol. 21, no. 13, pp. 14011–14026, Jul. 2021.

[16] K. R. Konnaiyan, S. Cheemalapati, M. Gubanov, and A. Pyayt, "MHealth dipstick analyzer for monitoring of pregnancy complications," *IEEE Sensors J.*, vol. 17, no. 22, pp. 7311–7316, Nov. 2017.

[17] S. Lee, D. O'Dell, J. Hohenstein, S. Colt, S. Mehta, and D. Erickson, "NutriPhone: A mobile platform for low-cost point-of-care quantification of vitamin B12 concentrations," *Sci. Rep.*, vol. 6, no. 1, p. 28237, Jun. 2016.

[18] B. Srinivasan, J. L. Finkelstein, D. O'Dell, D. Erickson, and S. Mehta, "Rapid diagnostics for point-of-care quantification of soluble transferrin receptor," *EBioMedicine*, vol. 42, pp. 504–510, Apr. 2019.

[19] S. C. Kim, U. M. Jalal, S. B. Im, S. Ko, and J. S. Shim, "A smartphone-based optical platform for colorimetric analysis of microfluidic device," *Sens. Actuators B, Chem.*, vol. 239, pp. 52–59, Feb. 2017.

[20] H. Karlsen and T. Dong, "Smartphone-based rapid screening of urinary biomarkers," *IEEE Trans. Biomed. Circuits Syst.*, vol. 11, no. 2, pp. 455–463, Apr. 2017.

[21] A. Mathaweesansurn, N. Maneerat, and N. Choengchan, "A mobile phone-based analyzer for quantitative determination of urinary albumin using self-calibration approach," *Sens. Actuators B, Chem.*, vol. 242, pp. 476–483, Apr. 2017.

[22] B. Coleman, C. Coarsey, and W. Asghar, "Cell phone based colorimetric analysis for point-of-care settings," *Analyst*, vol. 144, no. 6, pp. 1935–1947, Mar. 2019.

[23] A. Y. Mutlu, V. Kiliç, G. K. Özdemir, A. Bayram, N. Horzum, and M. E. Solmaz, "Smartphone-based colorimetric detection via machine learning," *Analyst*, vol. 142, no. 13, pp. 2434–2441, 2017.

[24] M. E. Solmaz, A. Y. Mutlu, G. Alankus, V. Kiliç, A. Bayram, and N. Horzum, "Quantifying colorimetric tests using a smartphone app based on machine learning classifiers," *Sens. Actuators B, Chem.*, vol. 255, pp. 1967–1973, Feb. 2018.

[25] R. J. Gove, "CMOS image sensor technology advances for mobile devices," in *High Performance Silicon Imaging*, Sawston, U.K.: Woodhead, 2020, pp. 185–240.

[26] Y. Jung, J. Kim, O. Awofeso, H. Kim, F. Regnier, and E. Bae, "Smartphone-based colorimetric analysis for detection of saliva alcohol concentration," *Appl. Opt.*, vol. 54, no. 31, pp. 9183–9189, Nov. 2015.

[27] S. Balbach, N. Jiang, R. Moreddu, X. Dong, W. Kurz, C. Wang, J. Dong, Y. Yin, H. Butt, M. Brischwein, O. Hayden, M. Jakobi, S. Tasoglu, A. W. Koch, and A. K. Yetisen, "Smartphone-based colorimetric detection system for portable health tracking," *Anal. Methods*, vol. 13, no. 38, pp. 4361–4369, Oct. 2021.

[28] Ö. B. Mercan, V. Kiliç, and M. Şen, "Machine learning-based colorimetric determination of glucose in artificial saliva with different reagents using a smartphone coupled μPAD," *Sens. Actuators B, Chem.*, vol. 329, Feb. 2021, Art. no. 129037.

[29] S. Bhatt, S. Kumar, M. K. Gupta, S. K. Datta, and S. K. Dubey, "Colorimetry-based and smartphone-assisted machine-learning model for quantification of urinary albumin," *Meas. Sci. Technol.*, vol. 35, no. 1, Jan. 2024, Art. no. 015030.
[30] V. Markus, O. Dalmizrak, O. H. Edebal, M. Al-Nidawi, and J. Caleb, "Smartphone digital image colorimetry for quantification of serum proteins," *Anal. Methods*, vol. 15, no. 38, pp. 5018–5026, Oct. 2023.
[31] S. Bianco, C. Cusano, and R. Schettini, "Color constancy using CNNs," in *Proc. IEEE Conf. Comput. Vis. Pattern Recognit. Workshops (CVPRW)*, Jun. 2015, pp. 81–89.
[32] Z. Yang, K. Xie, T. Li, Y. He, T. Li, and X. Sun, "Color constancy using VGG convolutional neural network," in *Proc. Int. Conf. High Perform. Big Data Intell. Syst. (HPBDIS)*, May 2020, pp. 1–6.
[33] T. Yuan and X. Li, "Full convolutional color constancy with adding pooling," in *Proc. IEEE 11th Int. Conf. Commun. Softw. Netw. (ICCSN)*, Jun. 2019, pp. 666–671.
[34] S. Sankaranarayanan, Y. Balaji, C. D. Castillo, and R. Chellappa, "Generate to adapt: Aligning domains using generative adversarial networks," in *Proc. IEEE/CVF Conf. Comput. Vis. Pattern Recognit.*, Jun. 2018, pp. 8503–8512.
[35] P. Isola, J.-Y. Zhu, T. Zhou, and A. A. Efros, "Image-to-image translation with conditional adversarial networks," in *Proc. IEEE Conf. Comput. Vis. Pattern Recognit. (CVPR)*, Jul. 2017, pp. 5967–5976.
[36] I. Goodfellow, J. Pouget-Abadie, M. Mirza, B. Xu, D. Warde-Farley, S. Ozair, A. Courville, and Y. Bengio, "Generative adversarial networks," *Commun. ACM*, vol. 63, no. 11, pp. 139–144, 2020.
[37] S. Fathi-Kazerooni and R. Rojas-Cessa, "GAN tunnel: Network traffic steganography by using GANs to counter internet traffic classifiers," *IEEE Access*, vol. 8, pp. 125345–125359, 2020.
[38] M. Mirza and S. Osindero, "Conditional generative adversarial nets," 2014, *arXiv:1411.1784*.
[39] V. A. Knyaz, V. V. Kniaz, and F. Remondino, "Image-to-voxel model translation with conditional adversarial networks," in *Proc. Eur. Conf. Comput. Vis. (ECCV) Workshops*, 2018, pp. 601–618.
[40] M. M. Almeida, J. D. S. de Almeida, G. B. Junior, A. C. Silva, and A. C. de Paiva, "Univariate time series missing data imputation using Pix2Pix GAN," *IEEE Latin Amer. Trans.*, vol. 21, no. 3, pp. 505–512, Mar. 2023.
[41] Z. Wang, A. C. Bovik, H. R. Sheikh, and E. P. Simoncelli, "Image quality assessment: From error visibility to structural similarity," *IEEE Trans. Image Process.*, vol. 13, no. 4, pp. 600–612, Apr. 2004.

SUNITA BHATT received the M.Tech. degree in applied optics from Indian Institute of Technology (IIT) Delhi, India. She is currently a Research Scholar with the Centre for Sensors, Instrumentation and Cyber-Physical System Engineering (SeNSE), IIT Delhi. Her research interests include smartphone-based imaging and bio-sensing for point-of-care diagnostics applications, microscopy, image processing, and machine learning.

SANDEEP KUMAR SINGH received the B.Tech. degree in mechanical engineering from the JSS Academy of Technical Education, Noida, India. He is currently pursuing the M.Tech. degree in instrument technology from the Centre for Sensors, Instrumentation and Cyber-Physical System Engineering (SeNSE), Indian Institute of Technology (IIT) Delhi, India.

SUNIL KUMAR received the master's degree in robotics engineering from the University of Petroleum and Energy Studies, Dehradun, India, in 2016, and the Ph.D. degree in robotics from the Dr. B. R. Ambedkar National Institute of Technology, Jalandhar, India. From 2016 to 2017, he was a Junior Research Fellow with the joint Indo-Korean Research Project. He is currently a Research Associate with the Centre for Sensors, Instrumentation and Cyber Physical System Engineering (SeNSE), Indian Institute of Technology (IIT) Delhi, New Delhi. His research interests include machine learning, compressive sensing, mobile robotics, shared autonomy, and artificial intelligence.

SUDIP KUMAR DATTA received the M.B.B.S. degree from Calcutta National Medical College, University of Calcutta, in 2002, and the M.D. degree in medical biochemistry from the University College of Medical Sciences (UCMS), University of Delhi, in 2010. He is currently an Associate Professor with the Department of Laboratory Medicine, All India Institute of Medical Sciences (AIIMS), New Delhi. He was an Assistant Professor with the Vardhaman Mahavir Medical College and the Safdarjung Hospital, New Delhi; and the Post Graduate Institute of Medical Education and Research (PGIMER), Chandigarh, prior to joining AIIMS, in 2014. He is also the Faculty In-Charge of clinical chemistry services with AIIMS. He has authored more than 20 original articles published in national and international journals and about 40 papers in conference proceedings. He is a Technical Assessor of Clinical Biochemistry with the National Accreditation Board for Calibration and Testing Laboratories (NABL), a Corresponding Member of the International Federation of Clinical Chemistry and Laboratory Medicine (IFCC) Task Force on Ethics (TF-E), an Associate Editor of *Journal of Laboratory Physicians*, a Secretary of American Association of Clinical Chemistry (AACC)-India Section, and an Executive Member of the Association of Medical Biochemists of India (AMBI) Delhi Chapter.

SATISH KUMAR DUBEY received the M.Tech. degree in applied optics and the Ph.D. degree from IIT Delhi, in 2004 and 2009, respectively. He was an Optics Engineer with Coherent, Singapore. He was a Scientist with the Central Scientific Instruments Organization, Chandigarh, and the Instrument Research and Development Establishment (IRDE), Dehradun, a unit of DRDO. Prior to joining IIT Delhi, he was a Technical Expert with the Corporate Research and Development Establishment, Siemens, Bengaluru, for six years, where he handled several research and development establishment projects. He has been an Associate Professor with SeNSE, IIT Delhi, since November 2016. He has published 35 research articles in international peer-reviewed journals, around 30 papers in conference proceedings, and 12 patent filings, including three granted patents. His research interests include electro-optic sensing and imaging, interferometry techniques, and spectroscopic instrumentation.